Preparation, Structures, and Properties of Dinuclear Ni and Pd Complexes of Tridentate Amine-Chalcogenolate Ligands

Berthold Kersting

Institut für Anorganische und Analytische Chemie, Universität Freiburg,
Albertstrasse 21, D-79104 Freiburg, Germany
Fax: (internat.) + 49(0)761/203-6001
E-mail: kerstber@sun2.ruf.uni-freiburg.de

Received March 27, 1998

Keywords: Dinuclear complexes / Nickel / Palladium / Amine-thiolate ligands/ Amine-selenolate ligands

The preparation and characterization of dinuclear Ni^{II} and Pd^{II} complexes of the tridentate amine-chalcogenolate ligands 4-*tert*-butyl-2,6-di(aminomethyl)thiophenol (**4a**) and 4-*tert*-butyl-2,6-di(aminomethyl)selenophenol (**4b**) are reported. Reaction of **4a**,**b** with $Ni(ClO_4)_2 \cdot 6\ H_2O$ or $(COD)PdCl_2$ in a 1:1 molar ratio yields 1:1 complexes of composition $[M_2(L)_2][BPh_4]_2 \cdot CH_3CN \cdot CH_3OH$ [M = Ni, L = **4a**,**b** (**5a**,**b**); M = Pd, L = **4a**,**b** (**6a**,**b**)]. The palladium complex **6a** is isomorphous with **5a** as shown by X-ray crystal structure analysis. NMR studies reveal that both complexes retain their solid-state structure in solution and that the selenolate complexes are isostructural with the thiolate complexes. All complexes undergo electrochemically reversible one-electron transfer processes in the potential range –1.0 to –0.8 V vs. SCE ascribed to metal-centered reductions with formation of mixed-valent $M^{I,II}$ species $[M_2(L)_2]^+$. Further reduction at more negative potentials then leads to the neutral $[M_2(L)_2]$ species, which are not stable on the time scale of the CV experiment. The spectroscopic properties of the thiolate and selenolate complexes are very similar indicating electronically similar properties of the tridentate amine-chalcogenolate ligands.

Introduction

The coordination chemistry of transition-metal thiolate, selenolate, and tellurolate complexes has been actively pursued in the past several years, motivated primarily by the bonding diversity[1][2], potential use as precursors to new solid-state materials[3], and the relevance of such complexes to biomimetic chemistry[4][5]. Monodentate chalcogenolate ligands, which have been studied most, form complexes with most of the elements, however, their inherent tendency to form bridges between transition-metal ions limits their use in the preparation of complexes of well-defined nuclearity[6]. Furthermore, an investigation of chemical reactivities is often hampered by ligand-centered redox reactions and the fact that such species can be notoriously labile[7].

More recently, multidentate nitrogen/sulfur-based ligands have been employed as spectator ligands in various mononuclear[8][9][10] and dinuclear transition-metal complexes[11][12] and have been shown to offer some unique properties in coordination chemistry. The notable feature of such complexes is their enormous stability that has enabled the preparation of complexes with metal ions in unusual high formal oxidation states[13][14] and has allowed for studies on their chemical reactivity[15]. However, while mononuclear complexes have been extensively studied, dinuclear complexes have been considered less often, and very little information is available on their reactivity[16][17]. This is true in particular for complexes with polydentate nitrogen/selenium-based ligands[18].

Scheme 1. Structures of amine-chalcogenolate ligands **4a**,**b** and the binding mode of **4a** in the dinuclear $[Ni_2(\mathbf{4a})_2]^{2+}$ dication in $[Ni_2(\mathbf{4a})_2][BPh_4]_2$ (**5a**)[20]

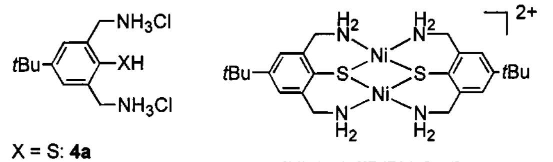

X = S: **4a**
X = Se: **4b**

$[Ni_2(4a)_2][B(Ph)_4]_2$, **5a**

Our work on thiolate-bridged dimetal complexes[19] has shown that the dinickel complex **5a** of the tridentate N_2S ligand **4a** is quite robust, tolerating binding of exogenous ligands without affecting the dinuclear structure[20]. Complex **5a** also serves as a versatile starting agent in the preparation of novel face-sharing bioctahedral nickel complexes. This prompted us to investigate the possibility of synthesizing related complexes with the amine-selenolate ligand **4b**.

This article describes the syntheses and characterization of dinuclear nickel and palladium complexes of the analogous ligands 2,6-bis(aminomethyl)-4-*tert*-butylthiophenol (**4a**) and 2,6-bis(aminomethyl)-4-*tert*-butylselenophenol (**4b**).

Results and Discussion

Syntheses

Compounds **4a**,**b** were prepared in 3 steps starting from **1**, as is shown in Scheme 2. In the first step, compound **1** was treated with potassium benzylthiolate in dimethylformamide to afford benzyl [4-*tert*-butyl-2,6-diformylphenyl]sulfide in nearly quantitative yield. The dialdehyde **2a** was subsequently converted to the corresponding dioxime **3a** by reaction with hydroxylamine. In the last step, reduction of compound **3a** was accomplished with sodium in liquid ammonia. The amine-thiolate compound **4a** was isolated as the hydrochloride salt **4a**$\cdot$(HCl)$_2$ in 55% overall yield. A similar reaction sequence was employed to prepare the selenium analogue **4b**.

Scheme 2. Preparation of amine-chalcogenolate ligands **4a**,**b**

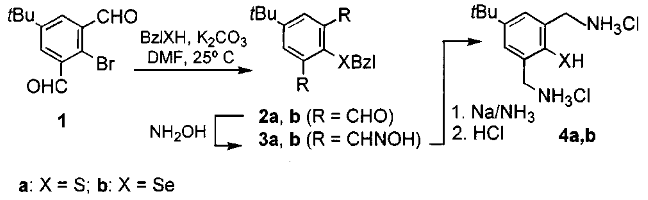

Metal Complex Syntheses

The hydrochloride salts of the chalcogenolate ligands **4a**,**b** react with equimolar quantities of $Ni(ClO_4)_2 \cdot 6H_2O$ in the presence of base to give the air-stable dications $[Ni_2(\mathbf{4a})_2]^{2+}$ and $[Ni_2(\mathbf{4b})_2]^{2+}$, respectively (eq. 1). These cationic species were isolated as the tetraphenyl borate salts $[Ni_2(\mathbf{4a})_2][BPh_4]_2$ (**5a**) and $[Ni_2(\mathbf{4a})_2][BPh_4]_2$ (**5b**). Complexes **5a**,**b** are dark-red crystalline solids, soluble in polar aprotic solvents like acetonitrile, dichloromethane, dimethyl sulfoxide, and dimethylformamide. Similarly, reaction of **4a**,**b** with (COD)PdCl$_2$ and NaOMe in methanol produced, upon addition of NaBPh$_4$, yellow crystals of the palladium analogs of **5a**,**b** in good yields {$[Pd_2(\mathbf{4a})_2][BPh_4]_2$ (**6a**), 82%; $[Pd_2(\mathbf{4b})_2][BPh_4]_2$ (**6b**), 63%}.

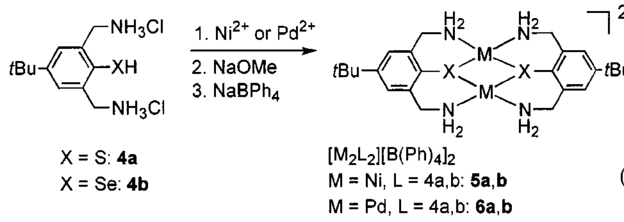

(1)

When recrystallized from acetonitrile/methanol solution, the complexes crystallize with a solvent molecule of acetonitrile and a solvent molecule of methanol per dication. The dinuclear nature of the complexes was confirmed by X-ray crystal structure determination of the palladium complex **6a** $\cdot$ CH$_3$CN $\cdot$ CH$_3$OH. The structure of **5a** $\cdot$ CH$_3$CN $\cdot$ CH$_3$OH has been determined previously[20].

Crystal Structure of 6a·CH$_3$CN·CH$_3$OH

The X-ray crystal structure determination of **6a** $\cdot$CH$_3$CN$\cdot$CH$_3$OH revealed the structure to consist of well-separated molecules of the dipalladium complex and two tetraphenylborate anions. The two solvent molecules of crystallization form hydrogen bonds with nitrogen atoms [N(1), N(3)] of the dication [N(1)−H(1B)···O(1) 2.892 A, N(3)−H(3A)···N(5) 3.307 A], but feature no bonding interactions with the palladium ions. **6a**$\cdot$CH$_3$CN$\cdot$CH$_3$OH is isomorphous and isostructural with **5a**$\cdot$CH$_3$CN$\cdot$CH$_3$OH. Although the dication does not possess crystallographically imposed symmetry, its idealized symmetry is C_{2v}. A perspective view of the molecular structure of the dipalladium complex with the atomic numbering scheme is shown in Figure 1.

Figure 1. Molecular structure of the $[Pd_2(\mathbf{4a})_2]^{2+}$ cation in **6a** (50% probability thermal ellipsoids)[a]

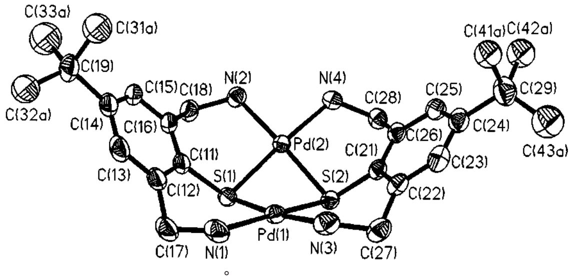

[a] Selected bond lengths [A] and angles [°]: Pd(1)−S(1) 2.3057(9), Pd(1)−S(2) 2.3020(11), Pd(1)−N(1) 2.076(3), Pd(1)−N(3) 2.076(3), Pd(2)−S(1) 2.3009(8), Pd(2)−S(2) 2.2951(9), Pd(2)−N(2) 2.069(2), Pd(2)−N(4) 2.084(2), Pd(1)···Pd(2) 3.0847(6); S(1)−Pd(1)−S(2) 81.79(3), S(1)−Pd(1)−N(1) 94.24(9), S(1)−Pd(1)−N(3) 173.56(8), S(2)−Pd(1)−N(1) 174.98(8), S(2)−Pd(1)−N(3) 94.34(8), N(1)−Pd(1)−N(3) 89.88(11), S(1)−Pd(2)−S(2) 82.05(3), S(1)−Pd(2)−N(2) 94.70(7), S(1)−Pd(2)−N(4) 175.48(7), S(2)−Pd(2)−N(2) 176.27(7), S(2)−Pd(2)−N(4) 93.78(7), N(2)−Pd(2)−N(4) 89.40(10).

As in the dinickel complex **5a**, the coordination of each Pd atom by two nitrogen and two bridging thiolate sulfur atoms is approximately planar. Maximum deviations from the least-squares planes defined by the atoms Pd(1), S(1), S(2), N(1), N(3) and Pd(2), S(1), S(2), N(2), N(4) are 0.078 and 0.028 A, respectively. The two planar PdN$_2$S$_2$ units are joined via two bridging thiolate atoms with a folding angle of 123.3° between the two planes. While this angle is only marginally smaller than the corresponding value in **5a** (124.6°), a larger difference is found for the angle between the two least-squares planes defined by the atoms of the phenyl rings of the two ligands (91.9° in **6a**, 96.1° in **5a**). The average Pd−N and Pd−S bond lengths are 2.076 and 2.301 A. In **5a**, the corresponding values were found to be 1.936 and 2.182 A, respectively. It is noted that the difference between Ni−N and Pd−N bond lengths (0.140 A) is larger than the difference in Ni−S and Pd−S bond lengths (0.119 A). Due to the longer Pd−S bonds in **6a**, the M···M distance within the dinuclear cations has increased from 2.973 A in **5a** to 3.085 A in **6a**.

In essence, the molecular structures of **6a** and **5a** show only slight differences. The most important information, however, is that both complexes are isomorphous and isostructural. The similar analytical and spectroscopic data of the complexes **5b** and **6b** (below) suggest that the selenolate complexes are also isomorphous and isostructural with the thiolate complexes.

NMR Spectroscopy

Complexes **5a**−**6b** have been examined by ^{1}H-NMR, ^{13}C{^{1}H}-NMR, and, where appropriate, by ^{77}Se-NMR spectroscopy. ^1H- and ^{13}C-chemical shifts and assignments according to Chart 1 are collected in Table 1.

Chart 1. ^1H-NMR labeling scheme

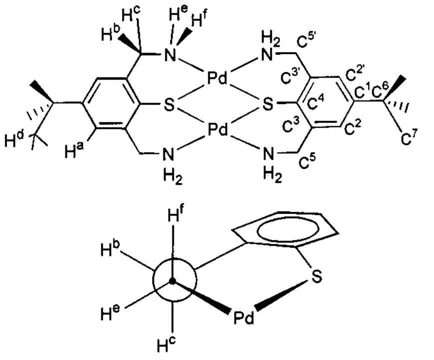

Figure 2. 200-MHz ^1H-NMR spectrum of **5b** in CD_2Cl_2 showing the four multiplets of the protons of the CH_2NH_2 groups in the region δ = 4.0−0.5 (*: resonances due to H_2O traces of the deuterated solvent)

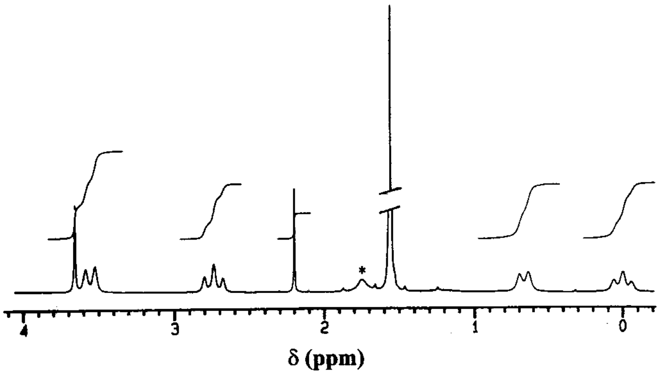

The ^1H-NMR spectrum of a solution of **6a** in CD_2Cl_2 is representative for all homodinuclear complexes **5a**−**6b**. Characteristic features are a singlet for the hydrogen atoms of the *tert*-butyl groups (H^d) at δ = 1.32 and a singlet for the hydrogen atoms bonded to the *meta*-carbon atoms of the phenyl ring (H^a) at δ = 7.24 (for **5a**,**b** this singlet is obscured by resonances of the anion). The signals of the methylene (H^b, H^c) and amine hydrogen atoms (H^e, H^f) of the aminomethyl groups appear as four multiplets centered at δ = 3.49, 3.11, 1.88, and 1.02. These form an ABCD spin system as evidenced by H,H-COSY spectroscopy, and this ABCD spin system in the alkane region is characteristic for all compounds (see Figure 2 for the spectrum of **5b**).

The vicinal coupling constants $|^3J_{b,f}|$, $|^3J_{b,e}|$, and $|^3J_{c,e}|$ were estimated (by graphical evaluation) to be less than 2 Hz, while $|^3J_{c,f}|$ was estimated to be ca. 12 Hz. Assignment of the amine hydrogen atoms was unambiguously achieved by an NH/ND-exchange experiment. Thus, addition of a few drops of a CD_3OD/D_2O (95:5) solution caused the two multiplets observed for H_e and H_f to disappear. Under these conditions the two multiplets observed for H_b and H_c now form an AB spin system (doublet of doublets). This allowed the geminal coupling constant of the methylene hydrogen atoms $^2J_{b,c}$ to be determined ($|^2J_{b,c}| \approx 12$ Hz). The two sets of vicinal coupling constants indicate a staggered conformation of the methylene and amine hydrogen atoms within the six-membered chelate ring similar to that observed in the solid state.

Table 1. ^1H- and $^{13}C\{^1H\}$-NMR spectroscopic data and assignments of complexes **5a**−**6b**[a]

	5a	**5b**	**6a**	**6b**
^1H NMR[b]				
H^a	[c]	[c]	7.24 (s, 4 H)	7.27 (s, 4 H)
H^b	3.19 (d, 4 H)	3.32 (d, 4 H)	3.49 (d, 4 H)	3.56 (d, 4 H)
H^c	2.62 (t, 4 H)	2.50 (t, 4 H)	3.11 (t, 4 H)	3.06 (t, 4 H)
H^d	1.31 (s, 18 H)	1.32 (s, 18 H)	1.32 (s, 18 H)	1.34 (s, 18 H)
H^e	0.51 (d, 4 H)	0.43 (d, 4 H)	1.88 (d, 4 H)	1.71 (d, 4 H)
H^f	−0.03 (t, 4 H)	−0.23 (t, 4 H)	1.02 (t, 4 H)	0.91 (t, 4 H)
$[BPh_4]^-$	7.57 (br. s, 16 H)	7.57 (br. s, 16 H)	7.57 (br. s, 16 H)	7.59 (br. s, 16 H)
	7.10 (m, 28 H)	7.10 (m, 28 H)	7.05 (t, 16 H)	7.06 (t, 16 H)
			6.90 (t, 8 H)	6.89 (t, 8 H)
CH_3OH[d]	3.37 (s, 3 H)	3.37 (s, 3 H)	3.37 (s, 3 H)	3.37 (s, 3 H)
CH_3CN[d]	1.97 (s, 3 H)	1.97 (s, 3 H)	1.97 (s, 3 H)	1.97 (s, 3 H)
^{13}C NMR				
C^1	152.7	153.3	152.5	151.1
C^2	135.2	137.4	136.2	140.4
C^3	128.3	128.3	129.5	128.6
C^4	121.9	118.3	125.6	123.2
C^5	45.8	47.9	48.1	48.8
C^6	34.9	34.9	34.8	34.5
C^7	30.8	30.9	30.8	31.0
$[BPh_4]^-$	164.0	164.1	164.2	162.0
	135.6	135.6	135.6	135.7
	126.9	126.9	126.8	125.5
	123.1	123.1	123.0	121.7
CH_3OH	50.1	49.9	50.0	50.1
CH_3CN	117.7	117.7	117.6	117.5
CH_3CN	1.7	1.7	1.6	1.3

[a] See Chart 1 for atom labeling; data are δ values. − [b] δ values for solutions of complexes in CD_2Cl_2. − [c] Obscured by resonances of $[BPh_4]^-$. − [d] Crystals of **5a**−**6b** slowly lose the acetonitrile and methanol molecules of crystallization upon storage in air at 298 K.

In the $^{13}C\{^1H\}$-NMR spectrum of **6a**, the $[Pd_2(\mathbf{4a})]^{2+}$ dication gives rise to four signals in the aromatic region and three signals in the aliphatic region again consistent with local C_{2v} symmetry of the dication in solution. The four signals in the aromatic region correspond to the *para*- (C^1), the *ipso*- (C^4), the *ortho*- (C^3, $C^{3'}$), and the *meta*-carbon atoms (C^2, $C^{2'}$) of the phenyl ring, whereas the singlets in the aliphatic region correspond to the quaternary carbon atom of the *tert*-butyl group (C^6), the three equivalent methyl carbon atoms of the *tert*-butyl group (C^7), and the methylene carbon atoms (C^5, $C^{5'}$).
Although the chemical shifts of the protons of the aminomethyl groups of the nickel complex **5a** are upfield from the corresponding resonances in the palladium complex **6a**, the otherwise identical ^{1}H-NMR and $^{13}C\{^1H\}$-NMR data clearly reveal that **6a** and **5a** retain their solid-state structure in solution. Furthermore, the similar ^{1}H-NMR and ^{13}C-NMR data of the selenolate complexes suggest that these are isostructural with the thiolate complexes. The singlet ^{77}Se resonance observed for **6b** at $\delta = 24.5$ also supports this assumption, however, for reasons unclear no ^{77}Se resonance was observed for **5b**.

It should also be noted that no exchange occurs between these dinuclear complexes in solution. When pure compounds were mixed in a ca. 1:1 ratio and investigated by ^{1}H-NMR spectroscopy, the spectra of such solutions resemble just superpositions of the spectra of the pure compounds. These spectra remained unchanged even after one week at room temperature. If exchange had occurred under these conditions, one would expect new signals due to mixed species such as $[Ni_2(\mathbf{4a})(\mathbf{4b})]^{2+}$ or $[NiPd(\mathbf{4a})_2]^{2+}$. These results demonstrate the stability of complexes **5a**−**6b**. The same conclusions can be drawn from the electrochemical studies presented below.

Infrared and UV/Vis Spectroscopy

Complexes **5a**−**6a** exhibit very similar IR spectra which are all dominated by two strong absorptions in the region 3350−3200 cm^{-1} (Table 2). These latter absorptions were assigned to $\nu_s(NH_2)$ and $\nu_{as}(NH_2)$ stretching vibrations of the CH_2NH_2 groups[21]. As is expected, the replacement of sulfur in **5a** or **6a** by selenium in **5b** or **6b** produces no shifts in $\nu(NH_2)$ stretching frequencies. However, the $\nu(NH_2)$ stretching modes in palladium complexes **6a**,**b** appear at higher frequencies than in nickel complexes **5a**,**b**. The increase in N−H stretching frequencies in Pd complexes **6a**,**b** reflects a stronger N−H bond consistent with longer Pd−N bonds and, therefore, less polarized N−H bonds in **6a**,**b**.

The UV/Vis spectra are also very similar. In each case two features appear in the region 320−380 nm, which are assigned to π-π* transitions of the ligands. The red color of the nickel complexes is due to the absorption maxima at 499 nm in **5a** and 509 nm in **5b**, which are assigned to chalcogenolate-to-Ni charge-transfer transitions. These bands are shifted to 426 nm in **6a** and 430 nm in **6b**. Relative to the positions of the charge-transfer transitions of the thiolate complexes, those of the selenolate complexes are slightly shifted to lower energy. This is in agreement with the principle of hard and soft acids and bases that classifies selenolate selenium atoms easier to polarize than thiolate sulfur atoms[22].

Table 2. Electrochemical, IR-spectroscopic, and UV/Vis data of complexes **5a**−**6b**

	5a	**5b**	**6a**	**6b**
Electrochemical data, $E^x_{1/2}$ [V][a]				
$E^1_{1/2}$	−0.97	−0.83	−1.02	−0.98
$E^2_{1/2}$	−1.48 (irr.)	−1.34 (irr.)	−1.51 (irr.)	−1.44 (irr.)
Infrared spectroscopic data, ν [cm^{-1}][b]				
$\nu_{as}(NH_2)$	3250 s	3248 s	3262 s	3263 s
$\nu_s(NH_2)$	3193 s	3197 s	3200 s	3201 s
UV/Vis data, λ_{max} [nm] (ε [M$^{-1}\cdot$cm^{-1}])[c]				
	320 (5629)	327 (5043)	318 (9593)	320 (10537)
	380 (7157)	389 (6741)	354 (8272)	354 (7210)
	499 (1713)	509 (1069)	426 (744)	430 (873)

[a] Experiments were carried out using DMF as the solvent with 0.1 M nBu$_4$NPF$_6$ as the supporting electrolyte, Pt disc working electrode and Pt wire auxiliary electrodes. All half-cell potentials were calibrated against an internal ferrocenium/ferrocene (Fc$^+$/Fc) standard; $E^x_{1/2} = (E^{ox}_p + E^{red}_p)/2$ for reversible one-electron transfer processes; oxidation (E^{ox}_p) or reduction peak potentials (E^{red}_p) are given for irreversible (irr.) processes. Reported values are referenced vs. SCE. − [b] As KBr pellets. − [c] Data recorded for solutions of **5a**,**b** in CH_2Cl_2 and **6a**,**b** in CH_3CN.

Electrochemistry

Cyclic voltammograms (CVs) of complexes **5a**−**6b** have been recorded in dimethylformamide solution containing 0.10 M tetra-*n*-butylammonium hexafluorophosphate as supporting electrolyte. All potentials are referenced to the SCE. The CV of **5b** is representative for all homodinuclear complexes **5a**−**6a** (Figure 3). The complex undergoes two irreversible reduction processes with cathodic peak potentials at −0.87 and −1.38 V vs. SCE (Table 2). However, when the scan is reversed at −1.2 V vs. SCE, the first reduction process becomes quasi-reversible with the appear-

Figure 3. Cyclic voltammogram of **5b** in DMF with 0.1 M nBu$_4$NPF$_6$ as supporting electrolyte, Pt disc working electrode, Pt wire auxiliary electrode, and Ag wire pseudo reference electrode; scan rate 200 mV·s^{-1}

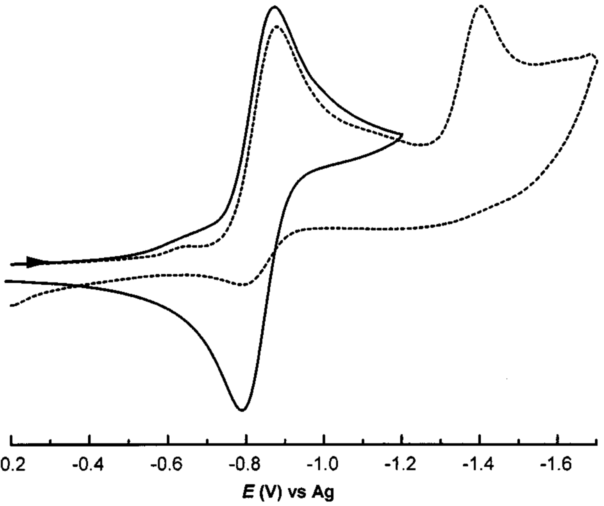

ance of an anodic peak at -0.76 V ($\Delta E^1 = 84$ mV). Reduction of **5b** at a constant potential of -1.2 V vs. SCE consumed 0.94 e^-/complex indicative of a one-electron transfer process. A similar electrochemical behaviour is observed for the other dinuclear complexes (Table 2).

Since the ligands in complexes **5a−6b** are unlikely to undergo ligand-centered redox reactions, it is concluded that all complexes undergo metal-centered redox reactions with the initial formation of mixed-valent $M^{II,I}$ monocations $[M_2(L)_2]^+$ (eq. 2). This is also supported by the electrochemical behaviour of related Ni and Pd complexes with planar $N_2(\mu_2\text{-}SR)_2$ coordination environments. The thiolate-bridged Ni^{II} complex $[Ni(pdmt)]_2$ (H_2pdmt = pyridine-2,6-dimethanethiol), for example, undergoes a one-electron reduction at $E_{1/2} = -1.21$ V vs. SCE ascribed to the formation of the mixed-valence $Ni^{II,I}$ complex $[Ni(pdmt)]_2^-$[23], while the trimetallic compounds $[(NiL')_2Ni]^{2+}$ and $[(NiL')_2Pd]^{2+}$ [L′ = 1,5-bis(mercaptoethyl)-1,5-diazacyclooctane] are reduced at -0.77 and -0.88 V vs. SCE, respectively[24]. It is noted that complexes **5a−6b** are readily reduced by $NaBH_4$ in THF to afford dark-brown solutions. These solutions are assumed to contain the respective mixed-valent $M^{I,II}$ monocations $[M_2(L)_2]^+$. However, any attempts to isolate the $M^{I,II}$ species have not yet been successful.

$$[M_2(L)_2]^{2+} + e^- \rightleftharpoons [M_2(L)_2]^+ \qquad (2)$$
$$(L = \mathbf{4a,b};\ M = Ni, Pd)\ E^1{}_{1/2}$$

Figure 4. Top: cyclic voltammogram of a solution containing **5a** and **6a** in a 1:1 molar ratio (solid line); bottom: square-wave voltammograms of a solution containing **5a** and **6a** in a 1:1 molar ratio (solid line) and of the same solution containing a slight excess of **6a** (dashed line)

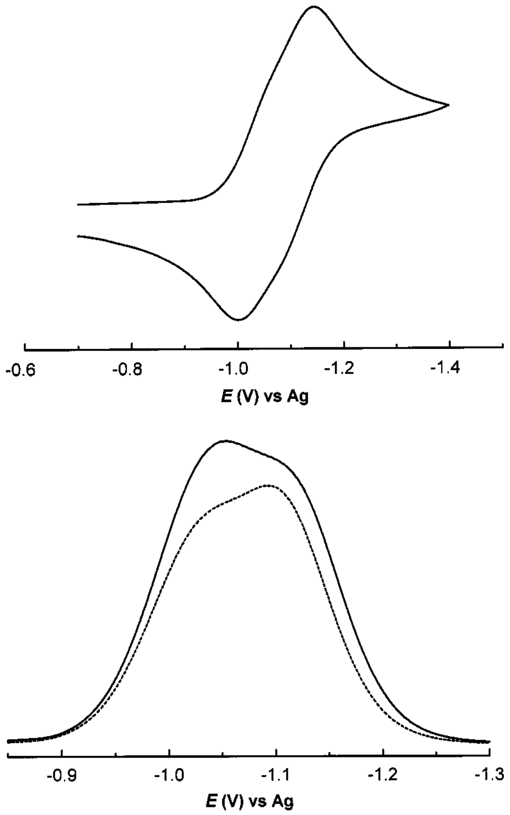

Table 2 shows that the redox potentials of the palladium complexes **6a**,**b** are only slightly shifted to more negative potentials when compared with those of the nickel complexes **5a**,**b**. Replacement of sulfur by selenium also does not dramatically shift the redox potentials, albeit both selenolate complexes are reduced at slightly less negative potentials than the thiolate complexes. It follows that the reduced species are equally well stabilized irrespective of the choice of N_2S_2 or N_2Se_2 coordination.

As previously established by NMR spectroscopy, the dinuclear complexes are quite stable in solution. These results are further confirmed by cyclic voltammetry. In Figure 4 (top), for example, is displayed the cyclic voltammogram of a mixture of complexes **5a** and **6a** in a 1:1 molar ratio in DMF solution. The CV reveals two overlapping reduction waves which correspond to independent reductions of **5a** and **6a**. Both reduction waves are clearly discernible in the corresponding square-wave voltammogram shown in Figure 4 (bottom).

In the present study it was shown that the tridentate amine-chalcogenolate ligands **4a**,**b** form dinuclear complexes with nickel and palladium. In contrast to many monodentate thiolate (or selenolate) ligands, the formation of complexes of higher or lower nuclearity was not observed. All complexes retain their solid-state structure in solution, where they do not undergo any exchange reactions. Furthermore, the existence as chalcogenolate-bridged dinuclear species in solution has allowed for reactivity studies. For example, all complexes undergo metal-centered electron-transfer reactions at potentials (-1.0 to -0.8 V vs. SCE) which are far more positive than those of mononuclear nickel or palladium complexes with N_2S_2 coordination environments ($E \approx -2.0$ V)[24]. Further studies will focus on the isolation, characterization, and an investigation of the chemical reactivity of these reduced species.

This work was supported by the *Deutsche Forschungsgemeinschaft*. The author thanks Prof. Dr. *H. Vahrenkamp* for his continuous and generous support and is grateful to Dipl.-Chem. *A. Trösch* for collecting the X-ray data.

Experimental Section

General: Dichloro(1,5-cyclooctadiene)palladium(II)[25], benzylselenol[26], and compound **5a**[20] were prepared according to literature procedures. Compound **1** was prepared by oxidation of 2-bromo-1,3-dimethyl-5-(1,1-dimethylethyl)benzene with CrO_3 in acetic anhydride[27]. All other chemicals were commercially available. The solvents were predried with molecular sieves and freshly distilled from appropriate drying agents. All reactions were carried out under dry nitrogen with standard Schlenk techniques. − CHN analyses: Perkin Elmer Elemental Analyzer 240. − IR: Bruker IFS25 spectrophotometer (KBr pellets). − ^1H NMR, $^{13}C\{^1H\}$ NMR: Bruker AC 200 spectrometer. − ^{77}Se NMR: Varian Unity 300 spectrometer. Dibenzyl diselenide was used as external standard. ^{77}Se NMR chemical shifts are referenced to Me_2Se_2[28]. − Absorption spectra: Jasco V-750 UV/VIS/NIR spectrometer. − Cyclic voltammetry: EG&G Princeton Applied Research Potentiostat/Galvanostat Model 263 A. The cell contained a Pt working electrode, a Pt wire auxiliary electrode, and an Ag wire pseudo reference electrode. Concentration of solutions were 0.1 M in supporting electrolyte ($n\mathrm{Bu_4NPF_6}$) and ca 1×10^{-3} M in sample. All potentials were scaled to ferrocenium/ferrocene as internal standard and converted to the SCE reference[29].

Benzyl (4-tert-Butyl-2,6-diformylphenyl)sulfide (**2a**): To a suspension of phenylmethanethiol (6.58 g, 53.0 mmol) and K_2CO_3 (8.29 g, 60.0 mmol) in DMF (80 ml) was added solid 1-bromo-4-*tert*-butyl-2,6-diformylbenzene (14.3 g, 53.0 mmol). After stirring the reaction mixture for 12 h, the crude product solidified upon dropwise addition of water (200 ml). The solid was isolated by filtration, washed with 100 ml of water, and dried in vacuum. The crude product was used without further purification, yield 15.4 g (93%), m.p. 78−80°C. − IR (KBr pellet): $\nu = 1720\ \mathrm{cm^{-1}}$ (CO). − ^{1}H NMR ($CDCl_3$): δ = 10.57 (s, 2 H, C*H*O), 8.13 (s, 2 H, aromatic H), 7.20-7.16 (m, 3 H, aromatic H), 6.86 (m, 2 H, aromatic *H*), 3.91 (s, 2 H, SC*H*$_2$), 1.35 (s, 9 H, C*H*$_3$). − ^{13}C{^{1}H} NMR ($CDCl_3$): δ = 191.3 (*C*HO), 153.5, 138.8, 137.4, 135.8, 130.4, 128.7, 128.6, 127.7, 43.7, 35.1, 30.8.

Benzyl (4-tert-Butyl-2,6-diformylphenyl)selenide (**2b**): Analogously to the preparation of **2a**, compound **2b** was prepared from phenylmethaneselenol (9.07 g, 53.0 mmol), K_2CO_3 (8.29 g, 60.0 mmol), and 1-bromo-4-*tert*-butyl-2,6-diformylbenzene (14.3 g, 53.0 mmol). The crude product was used without further purification, yield 16.6 g (87%), m.p. 79−81°C. − ^{1}H NMR ($CDCl_3$): δ = 10.51 (s, 2 H, C*H*O), 8.13 (s, 2 H, aromatic H), 7.16 (m, 3 H, aromatic H), 6.87 (m, 2 H, aromatic H), 3.93 (s, $^2J_{\mathrm{Se,H}}$ = 16 Hz, 2 H, SeC*H*$_2$), 1.36 (s, 9 H, C*H*$_3$). − ^{13}C{^{1}H} NMR ($CDCl_3$): δ = 193.0 (*C*HO), 153.3, 138.4, 136.6, 133.1, 130.3, 128.4, 128.3, 127.2, 35.2, 34.9, 30.7.

Benzyl [4-tert-Butyl-2,6-di(hydroximinoformyl)phenyl]sulfide (**3a**): To a suspension of $NH_2OH \cdot HCl$ (2.78 g, 40.0 mmol) in $CHCl_3$ (100 ml) was added a solution of NEt_3 (4.05 g, 40.0 mmol) in $CHCl_3$ (50 ml). A solution of compound **2a** (6.25 g, 20.0 mmol) in $CHCl_3$ (100 ml) was added, and stirring was continued for 12 h. The organic phase was washed with 200 ml of water, separated, and dried with $MgSO_4$. The solvent was removed in vacuum to afford a pale yellow crystalline residue. This material was recrystallized from benzene, colorless crystals, 5.96 g (87%). − ^{1}H NMR ([D$_6$]DMSO): δ = 11.41 (s, 2 H, O*H*), 8.55 (s, 2 H, C*H*), 7.82 (s, 2 H, aromatic H), 7.20 (m, 3 H, aromatic H), 7.02 (m, 2 H, aromatic H), 3.85 (s, 2 H, SC*H*$_2$), 1.29 (s, 9 H, C*H*$_3$). − ^{13}C{^{1}H} NMR ([D$_6$]DMSO): δ = 151.6, 146.9, 137.1, 136.9, 128.9, 128.7, 128.3, 127.2, 123.6, 41.3, 34.5, 30.8.

Benzyl [4-tert-Butyl-2,6-di(hydroximinoformyl)phenyl]selenide (**3b**): Analogously to the preparation of **3a**, compound **3b** was prepared from **2b** (7.19 g, 20.0 mmol), $NH_2OH \cdot HCl$ (2.78 g, 40.0 mmol), and NEt_3 (4.05 g, 40.0 mmol) in $CHCl_3$, colorless crystals, 6.62 g (85%). − ^{1}H NMR ([D$_6$]DMSO): δ = 11.37 (s, 2 H, O*H*), 8.52 (s, 2 H, C*H*), 7.79 (s, 2 H, aromatic H), 7.16 (m, 3 H, aromatic H), 7.00 (m, 2 H, aromatic H), 3.89 (s, $^2J_{\mathrm{Se,H}}$ = 16 Hz, 2 H, SeC*H*$_2$), 1.30 (s, 9 H, C*H*$_3$). − ^{13}C{^{1}H} NMR ([D$_6$]DMSO): δ = 151.5, 149.0, 138.0, 137.3, 128.4, 128.2, 126.8, 126.4, 123.6, 34.4, 33.4, 30.8.

2,6-Bis(aminomethyl)-4-tert-butylthiophenol (**4a**): A solution of **3a** (6.85 g, 20.0 mmol) in THF (50 ml) was added dropwise to a solution of sodium (6.05 g, 28.3 mmol) in liquid ammonia (100 ml). During addition the temp. was kept below −60°C by cooling with a dry ice/2-propanol bath. After the deep blue reaction mixture was stirred for further 3 h at −50°C, solid ammonium chloride was added to destroy excess reducing equivalents. After the ammonia was allowed to evaporate at atmospheric pressure, the remaining THF was evaporated in vacuum. The pale yellow solid was dissolved in 30 ml of water and the pH of the solution adjusted to 1 by addition of 1 M HCl. After stirring for 30 min, the precipitate was collected by filtration, and recrystallized from 1 M HCl to give 4.04 g (68%) of **4a**$\cdot$2HCl as pale yellow needles. − ^{1}H NMR (CD_3OD): δ = 7.65 (s, 2 H, aromatic H), 4.44 (s, 4 H, C*H*$_2$), 1.37 (s, 9 H, C*H*$_3$). − ^{13}C{^{1}H} NMR (CD_3OD): δ = 153.6, 138.1, 129.6, 127.6, 43.7, 36.1, 31.6.

2,6-Bis(aminomethyl)-4-tert-butylselenophenol (**4b**): Analogously to the preparation of **4a**, compound **4b** was prepared by reduction of **3b** (7.79 g, 20.0 mmol) with sodium in liquid ammonia. Recrystallization from 1 M HCl afforded 3.98 g (58%) of **4b**$\cdot$2HCl as yellow needles. − ^{1}H NMR (CD_3OD): δ = 7.68 (s, 2 H, aromatic H), 3.92 (s, 4 H, C*H*$_2$), 1.42 (s, 9 H, C*H*$_3$). − ^{13}C{^{1}H} NMR (CD_3OD): δ = 156.8, 139.6, 130.9, 129.9, 45.3, 36.2, 31.6.

Bis[2,6-bis(aminomethyl)-4-tert-butylselenophenolato]-dinickel(II) Tetraphenylborate·Acetonitrile·Methanol (**5b**): A solution of $Ni(ClO_4)_2 \cdot 6H_2O$ (731 mg, 2.00 mmol) in methanol (10 ml) was added to a solution of **4b**$\cdot$(HCl)$_2$ (688 mg, 2.00 mmol) in methanol (10 ml). After the pale yellow solution was stirred for 10 min, 12.0 ml of a 0.5 M solution of NaOMe in methanol (6.00 mmol) was added. To the dark red solution was added a solution of $NaBPh_4$ (856 mg, 2.50 mmol) in methanol (2 ml). After the mixture was allowed to stand overnight, the microcrystalline residue was collected by filtration, washed with methanol (3 × 5 ml), and dried in air. The crude product was recrystallized from CH_3CN/MeOH (1:1), dark-red crystals, 1.07 g (78%), m.p. 206−209°C (decomp.). − $C_{72}H_{78}B_2N_4Ni_2Se_2 \cdot CH_3CN \cdot CH_3OH$ (1369.45): calcd. C 65.78, H 6.26, N 5.11; found C 65.46, H 6.30, N 4.84.

Bis[2,6-bis(aminomethyl)-4-tert-butylthiophenolato]-dipalladium(II) Tetraphenylborate·Acetonitrile·Methanol (**6a**): A solution of (COD)$PdCl_2$ (571 mg, 2.00 mmol) in methanol (10 ml) was added to a solution of **4a**$\cdot$(HCl)$_2$ (595 mg, 2.00 mmol) in methanol (10 ml). After the pale yellow solution was stirred for 10 min, 12.0 ml of a 0.5 M solution of NaOMe in methanol (6.00 mmol) was added. To the dark-yellow solution was added a solution of $NaBPh_4$ (856 mg, 2.50 mmol) in methanol (2 ml). After the mixture was allowed to stand overnight, the microcrystalline residue was collected by filtration, washed with methanol (3 × 5 ml), and dried in air. The crude product was recrystallized from CH_3CN/MeOH (1:1), yellow crystals, 1.12 g (82%), m.p. 207−209°C (decomp.). − $C_{72}H_{78}B_2N_4Pd_2S_2 \cdot CH_3CN \cdot CH_3OH$ (1371.11): calcd. C 65.70, H 6.25, N 5.11; found C 65.39, H 6.27, N 5.02.

Bis[2,6-bis(aminomethyl)-4-tert-butylselenophenolato]-dipalladium(II) Tetraphenylborate·Acetonitrile·Methanol (**6b**): Analogously to the preparation of **6a**, compound **6b** was prepared from **4b** (688 mg, 2.00 mmol), (COD)$PdCl_2$ (571 mg, 2.00 mmol), 0.5 M NaOMe (12.0 ml, 6.00 mmol), and $NaBPh_4$ (855 mg, 2.50 mmol) in MeOH. The crude product was recrystallized from CH_3CN/MeOH (1:1), yellow crystals, 0.93 g (63%), m.p. 208−210°C (decomp.). − ^{77}Se NMR ([D$_6$]DMSO, 200 MHz): δ = 24.5. − $C_{72}H_{78}B_2N_4Pd_2Se_2 \cdot CH_3CN \cdot CH_3OH$ (1464.91): calcd. C 61.49, H 5.85, N 4.78; found C 61.43, H 6.03, N 4.72.

Crystal-Structure Determination: Crystals of **6a** suitable for X-ray structure analysis were obtained by recrystallization from an acetonitrile/methanol (1:1) solution. A yellow crystal of approximate dimensions 0.30 × 0.30 × 0.40 mm was selected and mounted on a glass fibre with a small amount of perfluoroether oil. After optical alignment at 193 K on an Enraf Nonius CAD4 diffractometer, the unit cell was determined from a least-squares fit of the setting angles of 25 carefully centered high-angle reflections. Crystal data and refinement details: $C_{75}H_{85}B_2N_5Pd_2OS_2$, M_r = 1371.11, monoclinic, space group $P2_1/n$, a = 22.130(4), b = 13.806(3), c = 23.672(5) A, β = 109.81(3)°, V = 6804.4 A^3, Z =

4, $\rho_{calcd.} = 1.34\ g\cdot cm^{-3}$, $\mu(Mo\text{-}K_{\alpha}) = 0.64\ mm^{-1}$, empirical absorption correction, transmission factors 0.89–0.98, 14383 reflections collected, 13297 unique reflections ($R_{int} = 0.0233$), 11448 observed reflections [$I > 2\sigma(I)$]. The structure was solved by direct methods (SHELXS-86)[30] and refined by full-matrix least-squares techniques against F^2 (SHELX-93). All non-hydrogen atoms were refined anisotropically except for the methyl carbon atoms of the disordered *tert*-butyl groups, which were refined isotropically. Hydrogen atoms were placed at calculated positions and were refined using a riding model with isotropic thermal parameters fixed at 1.2 times the equivalent isotropic U of the atom to which they were bonded. An isotropic split-atom model was applied for the disordered methyl carbon atoms. The multiplicities of the respective orientations C(31A)–C(33A), C(31B)–C(33B), C(41A)–C(43A), C(41B)–C(43B) were refined as follows: 0.58, 0.42, 0.51, 0.49. Final residuals: $R1$, $wR2$ [$F_o > 4\sigma(F_o)$]: 0.0369, 0.0955, $R1$, $wR2$ (all data): 0.0473, 0.1047, goodness-of-fit on F^2: 1.07, residual electron density: 0.771/–0.836 eA^{-3}. Crystallographic data (excluding structure factors) for the structure reported in this paper have been deposited with the Cambridge Crystallographic Data Centre as supplementary publication no. CCDC-101312. Copies of the data can be obtained free of charge on application to CCDC, 12 Union Road, Cambridge CB2 1EZ, UK [Fax: int. code + 44(1223)336-033; E-mail: deposit@cam.ac.uk].

---

[1] B. Krebs, G. Henkel, *Angew. Chem.* **1991**, *105*, 785–804; *Angew. Chem. Int. Ed. Engl.* **1991**, *30*, 769–788.

[2] J. Arnold, *Prog. Inorg. Chem.*, **1995**, *43*, 353–417.

[3] M. G. Kanatzidis, S. Huang, *Coord. Chem. Rev.* **1994**, *130*, 509–621.

[4] A. Volbeda, E. Garcin, C. Piras, A. L. de Lacey, V. M. Fernandez, E. C. Hatchikian, M. Frey, J. C. Fontecilla-Camps, *J. Am. Chem. Soc.* **1996**, *118*, 12989–12996.

[5] M. K. Eidsness, R. A. Scott, B. C. Prickril, D. V. DerVartanian, J. LeGall, I. Moura, J. J. G. Moura, H. D. Peck, *Proc. Natl. Acad. Sci. USA*, **1989**, *86*, 147–151.

[6] I. G. Dance, *Polyhedron* **1986**, *5*, 1037–1104.

[7] M. Kumar, R. O. Day, G. J. Colpas, M. J. Maroney, *J. Am. Chem. Soc.* **1989**, *111*, 5974–5976.

[8] D. Sellmann, W. Prechtel, F. Knoch, M. Moll, *Z. Naturforsch.* **1992**, *47b*, 1411–1423.

[9] T. Beissel, K. S. Bürger, G. Voigt, K. Wieghardt, C. Butzlaff, A. X. Trautwein, *Inorg. Chem.* **1993**, *32*, 124–126.

[10] D. K. Mills, J. H. Reibenspies, M. Y. Darensbourg, *Inorg. Chem.* **1990**, *29*, 4364–4366.

[11] T. Beissel, T. Glaser, F. Kesting, K. Wieghardt, B. Nuber, *Inorg. Chem.* **1996**, *35*, 3936–3947.

[12] [12a] A. J. Atkins, A. J. Blake, M. Schröder, *J. Chem. Soc., Chem. Commun.* **1993**, 1662–1665. – [12b] A. J. Atkins, D. Black, A. J. Blake, A. Marin-Becerra, S. Parsons, L. Ruiz-Ramirez, M. Schröder, *J. Chem. Soc., Chem. Commun.* **1996**, 457–464.

[13] [13a] D. Sellmann, S. Emig, F. W. Heinemann, *Angew. Chem.* **1997**, *109*, 1808–1810; *Angew. Chem. Int. Ed. Engl.* **1997**, *36*, 1734–1736. – [13b] D. Sellmann, S. Emig, F. W. Heinemann, F. Knoch, *Angew. Chem.* **1997**, *109*, 1250–1252; *Angew. Chem. Int. Ed. Engl.* **1997**, *36*, 1201–1203.

[14] [14a] J. Hanss, H.-J. Krüger, *Angew. Chem.* **1996**, *108*, 2989–2991; *Angew. Chem. Int. Ed. Engl.* **1996**, *35*, 2827–2830. – [14b] J. Hanss, H.-J. Krüger, *Angew. Chem.* **1998**, *110*, 366–369; *Angew. Chem. Int. Ed.* **1998**, *37*, 360–363.

[15] D. Sellmann, M. Hannakam, F. Knoch, M. Moll, *Z. Naturforsch.* **1992**, *47b*, 1545–1550.

[16] D. Sellmann, W. Soglowek, F. Knoch, M. Moll, *Angew. Chem.* **1989**, *101*, 1244–1245; *Angew. Chem. Int. Ed. Engl.* **1989**, *28*, 1271–1272.

[17] S. Brooker, P. D. Croucher, *J. Chem. Soc., Chem. Commun.* **1997**, 459–460.

[18] C. M. Goldman, M. M. Olmstead, P. K. Mascharak, *Inorg. Chem.* **1996**, *35*, 2752–2757.

[19] B. Kersting, M. J. Kolm, C. Janiak, *Z. Anorg. Allg. Chem.* **1998**, *624*, 775–780.

[20] B. Kersting, D. Siebert, *Inorg. Chem.*, in press.

[21] K. Nakamoto, *Infrared and Raman Spectra of Inorganic and Coordination Compounds*, Wiley, New York, **1978**.

[22] R. G. Pearson, *Survey Prog. Chem.* **1969**, *5*, 1–52.

[23] H.-J. Krüger, R. H. Holm, *Inorg. Chem.* **1989**, *28*, 1148–1155.

[24] G. Musie, P. J. Farmer, T. Tuntulani, J. H. Reibenspies, M. Y. Darensbourg, *Inorg. Chem.* **1996**, *35*, 2176–2183.

[25] D. Drew, J. R. Doyle, *Inorg. Synth.* **1972**, *13*, 47–55.

[26] H. J. Reich, C. P. Jasperse, J. M. Renga, *J. Org. Chem.* **1986**, *51*, 2981–2988.

[27] M. Tashiro, T. Yamato, *J. Chem. Soc., Perkin Trans. 1* **1979**, 176–179.

[28] R. K. Harris, B. E. Mann, *NMR and the Periodic Table*, Academic Press, London, **1978**.

[29] For formal potentials of the ferrocenium/ferrocene couple vs. SCE, see: N. G. Connelly, W. E. Geiger, *Chem. Rev.* **1996**, *96*, 877–910. Under our experimental conditions, the couple ferrocenium/ferrocene (Fc^+/Fc) is at $E_{1/2} = 0.45$ V (DMF, CH_2Cl_2) and $E_{1/2} = 0.40$ V (CH_3CN) vs. Ag.

[30] G. M. Sheldrick, *SHELXS-86*, University of Göttingen, Germany, **1990**; G. M. Sheldrick, *SHELXL-93,* University of Göttingen, Germany, **1993**.

[98084]